

The effect of grain refinement on the mechanical properties of a micro alloyed steel

M.A. Suarez^a, O. Alvarez^a, M. A. Alvarez-Pérez^a, R. Herrera^b, C. Zorrilla^b, S. Valdez^c, and J. A. Juárez-Islas^{a,*}

^aInstituto de Investigaciones en Materiales,

*e-mail: julioalb@servidor.unam.mx;

tel: (55)56224645

^bInstituto de Física,

^cInstituto de Ciencias Físicas, Universidad Nacional Autónoma de México,
Circuito Escolar S/N, Cd. Universitaria, 04510, México, D.F., México.

Recibido el 13 de abril de 2012; aceptado el 1 de agosto de 2012

High strength low alloy steel was produced by electric arc furnace, vacuum degassing, ladle treatment and continuous casting route. The steel was hot rolled by applying a schedule to simulate industrial control of hot rolling procedure for the production of plates as closely as possible in laboratory level, in order to investigate the effect of applying different strain rates onto hot rolling procedure in the range of temperatures between 1250 to 900°C. After the hot rolling procedure, the plate was spray cooled at a cooling rate of 5°C/s to a temperature of 650°C and then cooled to room temperature. The results showed a grain refinement as a function of the strain rate increases from 1 to 8 s⁻¹ and as a consequence an increase in mechanical properties of: yield strength and ultimate tensile strength; and keeping almost constant the ductility.

Keywords: Structural steel; strain rate; hot rolling; grain size; mechanical properties.

PACS: 61.66.D; 81.20.G; 81.60.B; 61.72.M; 62.20.F

1. Introduction

High strength low alloy (HSLA) steels for structural and pipeline applications are now produced by thermomechanical controlled rolling and spray cooling processes [1]. The increased strength of HSLA steels has been associated with different strengthening mechanism; one of the most important is the grain refinement, which can be obtained by the control of the rolling condition and by the addition of small quantities of micro alloying elements which improve both strength and toughness at the same time [2]. It can be mentioned, that the chemistry of pipeline steels needs to be redesigned, such that, it responds to the control of the thermomechanical processing, which is applied to steel slabs to produce an appropriated microstructure through the control of the recrystallization effect and transformation process.

During rolling together with a cooling procedure, just after the last finish of hot rolling pass, it is possible to achieve the required yield strength and toughness of modern pipelines steels demanded by the oil and gas industry [3-6]. The main focus of this work is to present results on the response of a Fe-C-Mn-Nb slab of steel to a controlled hot rolling schedule using different rolling strain rates followed by spray cooling on hot rolled plate in function of the resulting microstructure, grain size refinement and mechanical properties.

2. Experimental procedures

The composition of the steel under study is shown in Table I. It was obtained by feeding 100% sponge iron to an electric arc furnace, deslagging and poured into a ladle furnace at a temperature of 1680°C for secondary refinement. The process also includes vacuum degassing and continuous

casting. The controlled hot rolling procedure was performed on a Fenn reversible mill (0.127 m roll, 25 tones of load and 0.17 m/s of rolling speed).

Samples of 0.030×0.010×0.30 m were heated at 1250°C, at a heating rate of 0.4°C/s, soaked for 90 minutes and immediately hot rolled as shown schematically in Fig. 1. In order to control the temperature during the rolling and cooling operations, a Pt/Pt-13% Rh thermocouple was welded to one end of each specimen.

The rough rolling of the slab was performed from 1250°C to 1098°C in 5 passes, reaching 46 % of total deformation. This operation was followed by a cooling period until a temperature of 1050°C was reached; this temperature was fixed regarding the solubility of niobium carbonitride in austenite as reported in reference [7]. The final rolling procedure started at 1050°C and ended at 890°C, achieving a total deformation of 42% in 5 passes. During the hot rolling experiments, rolling strain rates of 1, 3 and 8 s⁻¹ were separately tested for each rate employed. Immediately after the last final rolling pass, the plates were spray cooled at a cooling rate of 5°C/s until a temperature of 650°C was reached and then, the plates were let to cool in air until room temperature.

TABLE I. Chemical composition of the steel under study (in wt. %)

C	Si	Mn	P	S	Cr	Ni
0.044	0.271	1.69	0.0091	0.0016	0.0103	0.240
V	Cu	Mo	Al	B	Nb	Ti
0.0010	0.2170	0.25	0.0310	0.0001	0.0554	0.014
Sn	As	Pb	Sb	Ca	N ₂	Ceq
0.0070	0.005	0.0018	0.0037	0.0016	0.0040	0.40

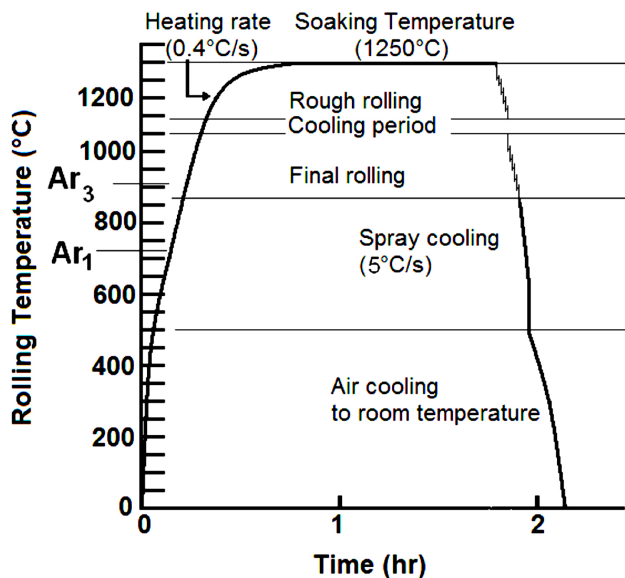


FIGURE 1. Heating, soaking and rolling of the slabs and cooling of the plates, where Ar_1 is the temperature at which transformation of austenite to ferrite or to ferrite plus cementite is completed during cooling and Ar_3 is the temperature at which austenite begins to transform to ferrite during cooling.

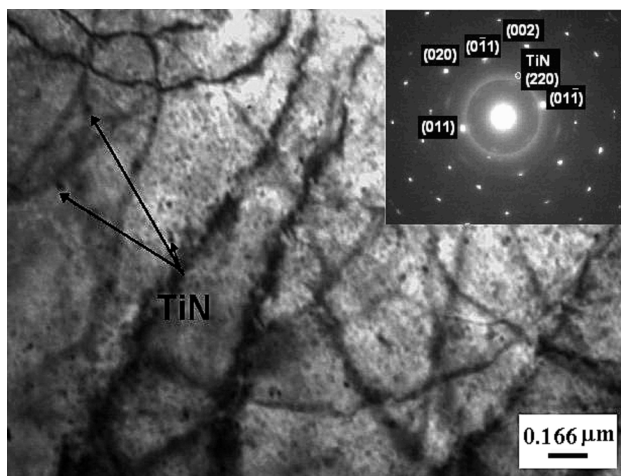


FIGURE 2. As-cast microstructure of the steel under study; the inset shows the electron diffraction pattern (EDP) of TiN precipitates in α -Fe matrix.

Microstructure of resulting plates was observed under a scanning electron microscope Stereoscan 440 and a scanning transmission electron microscope Jeol 2100, both microscopes were equipped with EDAX microanalysis. The Flat tensile (ASTM E-8) tests were conducted on an Instron 1125 (10 ton) test machine, employing only a strain rate of $5 \times 10^{-3} \text{ s}^{-1}$ at room temperature. Charpy V notch tests were performed according to ASTM A370 at room temperature. An optical microscope coupled to an image analyzer was used for quantitative determination of grain size, and volume fraction of bainite, which was carried out by measuring 10 fields per sample at 100 X. This accounted for a total analyzed area of about 6 mm^2 per specimen.

3. Results and discussion

Scanning electron microscopic observations carried out in the slab revealed a microstructure which consisted mainly of ferrite grains with some TiN precipitates as is shown in Fig. 2, these TiN precipitates showed a size $\leq 10 \text{ nm}$.

The microstructure of a slab after being hot rolled at a strain rate of 1 s^{-1} and the resulting plate accelerated to cool at $5^\circ\text{C}/\text{sec}$ is shown in Fig. 3a. As can be observed, the microstructure consisted of bainite hot bands $25 \mu\text{m}$ wide with a bainite grain size of $12 \mu\text{m}$, while Fig. 3b shows some bainite feathers where it is observed the presence of precipitates which were identified by STEM-microanalysis and diffracting patterns (EDP) as Cr_{23}C_6 and $\text{Nb}(\text{C},\text{N})$.

In Fig. 4a, it is shown the microstructure of a slab after being hot rolled at a strain rate of 3 s^{-1} and the resulting plate accelerated to cool at $5^\circ\text{C}/\text{sec}$. The microstructure consisted of bainite hot bands $20 \mu\text{m}$ wide with a bainite grain size of $9 \mu\text{m}$. In Fig. 4b, it is shown the bainite microstructure where it is observed some precipitates of $\text{Nb}(\text{C},\text{N})$ identified by STEM microanalysis and diffracting pattern shown in the inset of Fig. 4b.

Figure 5a shows the microstructure of a slab after being hot rolled at a strain rate of 8 s^{-1} and the resulting plate accelerated to cool at $5^\circ\text{C}/\text{sec}$. The microstructure consisted of bainite hot bands $15 \mu\text{m}$ wide with a bainite grain size refinement of $4 \mu\text{m}$. In Fig. 5b, it is shown the bainite grains with precipitates of $\text{Nb}(\text{C},\text{N})$ in the matrix and grain boundaries.

Regarding microstructure, in the as-cast slab, it was observed the presence of rectangular/cuboids of TiN precipitates. Garcia and coworkers [8] have observed these kind of larger size particles (size range up to $3 \mu\text{m}$) and identified them as almost pure TiN. On the other hand, in bainite feathers, it was observed the presence of precipitates which were identified by STEM microanalysis as Cr_{23}C_6 and $\text{Nb}(\text{C},\text{N})$. These precipitates showed an average particle size of around 10 nm . Akhlaghi [9] and Ghosha [10] studied the structure and properties of high strength low alloy steels, and under similar cooling conditions they reported the presence of NbC and/or NbN , in agreement with our results.

Table II shows the mechanical properties reached after hot rolled of slabs at different controlled strain rates plus accelerated cooling. As can be observed and with reference to the target properties, the hot rolling procedure accompanied by the cooling of plates by means of an accelerated cooling procedure, reached target properties equivalent to an API X-80 steel grade.

Also as has been mentioned [11], state of the art HSLA steels have a minimum yield strength of 550 MPa and are usually micro alloyed with Ti and Nb, where Ti levels are high enough to form TiN to remove the N from solid solution and the excess of Ti is available to enhance precipitation strengthening of fine carbides formed by the micro alloying elements. Nb additions play a critical role in delaying recrystallization during the last stage of the hot rolling procedure.

TABLE II. Mechanical properties of plates cooled in different media.

Strain rate (s^{-1})	0.2%YS		UTS		Elongation (%)	Charphy		Grain Size (μm)
	(MPa)	(Ksi)	(MPa)	(Ksi)		(Ft-Lb)	(J)	
1	600	87.0	738	107.0	21.5	85	115	12
3	624	90.5	767	111.2	21.1	79	107	9
8	638	92.5	785	113.8	20.7	75	102	4
Target	(552-655)	(80-95)	(621-690)	(90-100)	20 min	78	105	

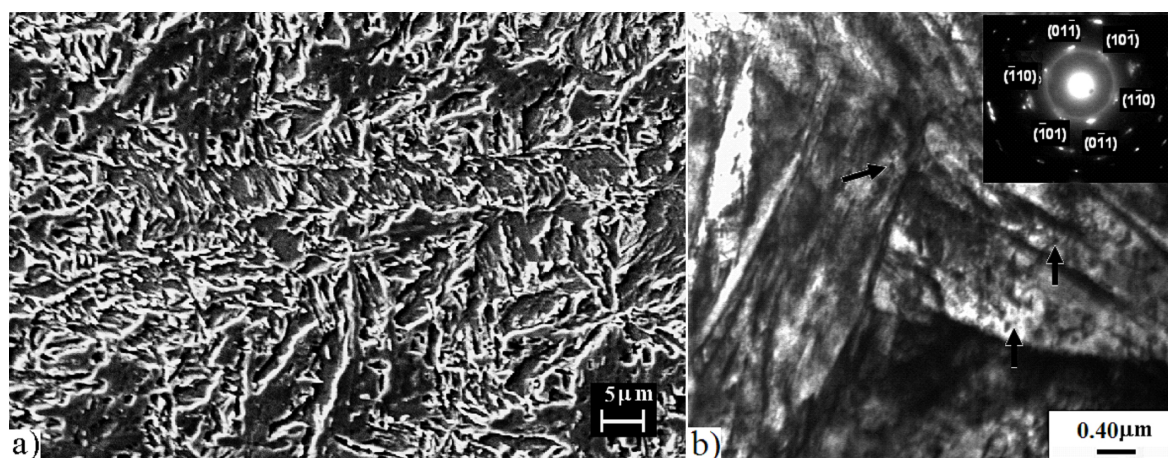


FIGURE 3. a) Bainite microstructure obtained after hot rolled of the slab at a strain rate of $1 s^{-1}$ and accelerated cooling of the plates at $5^{\circ}C/s$ with a grain size refinement of $12 \mu m$; b) Inset shows the EDP with axe zone $[1,0,0]$ of small precipitates of $Cr_{23}C_6$ into bainite feathures (shown by arrows).

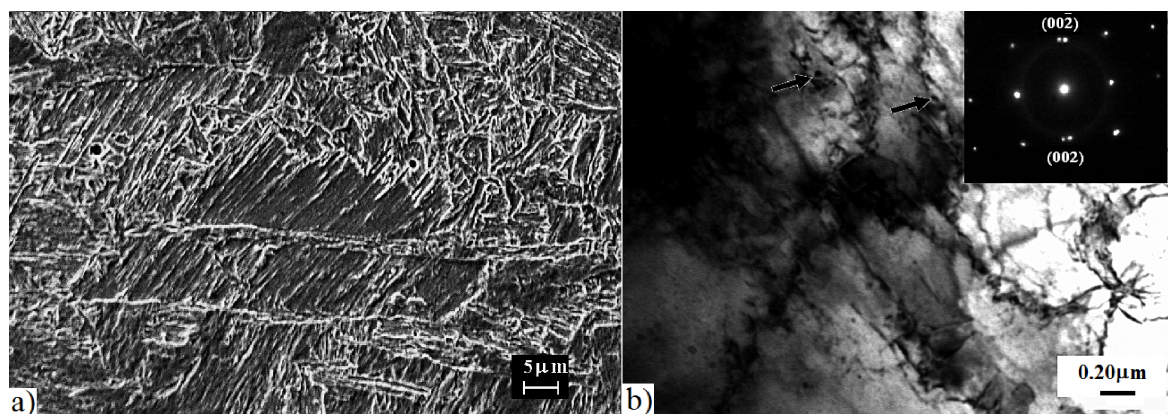


FIGURE 4. a) Bainite microstructure obtained after hot rolled of the slab at a strain rate of $3 s^{-1}$ and accelerated cooling of the plates at $5^{\circ}C/s$ with a grain size refinement of $9 \mu m$; b) Inset shows the EDP with axe zone $[3,2,0]$ of small precipitates of $Nb(C,N)$ in to bainite grains in matrix and grain boundaries (shown by arrows).

In this work, both Ti and Nb were observed as TiN and Nb(C,N) precipitates with a cubic and a more or less spherical morphology, respectively.

The optimum ratio of Ti:N or best grain refinement has been suggested to be close to the stoichiometry value of 3.42:1 [12], and in this work a Ti:N ratio of 3.5:1 was achieved. Regarding the addition of Nb, it has a profound effect on the improvement of properties through grain refinement and precipitation hardening [13]. In order to obtain

these desirable beneficial effects, it is necessary to dissolve the Nb(C,N) during reheating of the slab and then to control its precipitation properly in the subsequent rolling and cooling process [14,15]. Here the precipitation of Nb(C,N) was controlled during the thermomechanical processing of the slab by initiating the final rolling procedure at around $1051^{\circ}C$, taking into account the Nb, C and N contents of the steel.

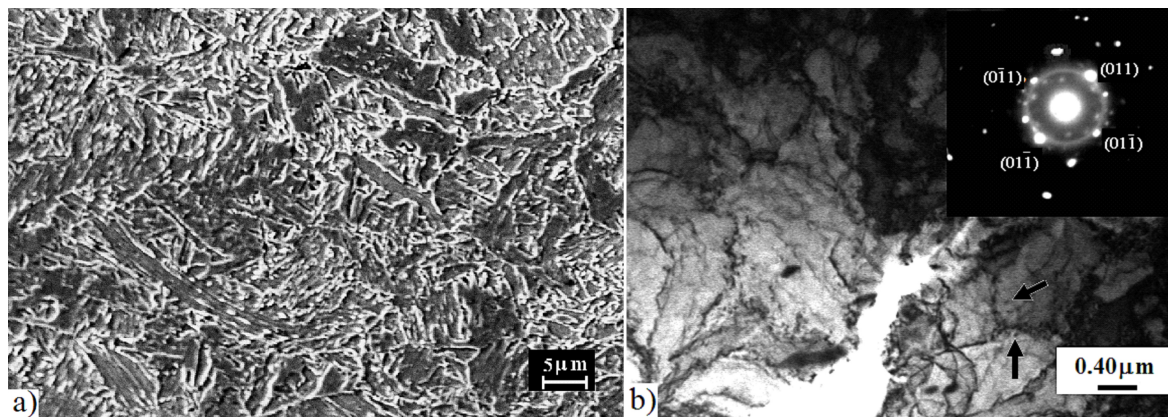


FIGURE 5. a) Bainite microstructure obtained after hot rolled of the slab at a strain rate of 8 s^{-1} and accelerated cooling of the plates at 5°C/s with a grain size refinement of $4 \mu\text{m}$; b) Inset shows the EDP with axe zone $[1,0,0]$ of Nb(C;N) precipitates in matrix and grain boundaries (shown by arrows).

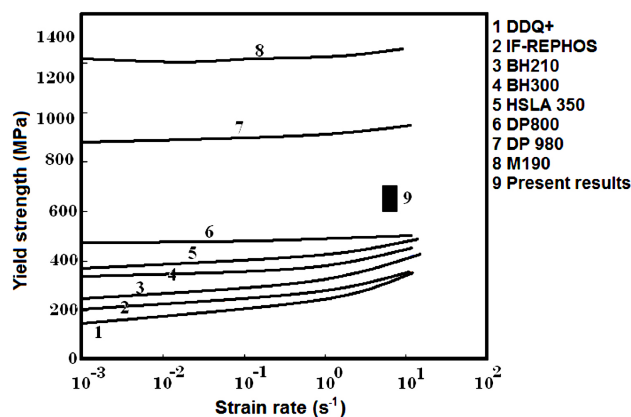


FIGURE 6. Yield strength as a function of strain rate.

Regarding the steel grade under development, it can be mentioned that the target properties of the resulting high-strength ferrite-bainite steel were achieved through the application of a thermomechanically controlled hot rolling schedule employing a strain rate of 8 s^{-1} , followed by an accelerated cooling procedure ensuring values of 0.2% YS of 638 MPa, 785 MPa of UTS, 20.7 % of elongation and 75 Ft-Lb of absorbed energy due to a contribution of grain size refinement, solid solution hardening, dislocation hardening, precipitation strengthening and transformation hardening.

Finally, Fig. 6 shows the behavior of yield strength as a function of strain rate for several HSLA alloy steels including the steel reported in this study. As expected, yield strength values show positive strain rate dependence while

the increase of yield strength with strain rate is slightly higher for steels of lower strength and is also higher at higher strain rates ($>1/\text{s}$). On the other hand, as can be observed in Fig. 6, by applying a controlled thermomechanical processing followed by an accelerated cooling procedure to an HSLA steel, it was possible to obtain higher properties than DP-steels.

4. Conclusions

1. The chemical composition of the steel under study responded positively to the controlled thermomechanical processing and the applied cooling media allowing to reach target properties equivalent to a steel API X-80 5L grade and higher properties as compared with some DP-steels.
2. The yield strength as a function of strain rate showed a positive strain rate dependence, increasing the yield strength as the strain rates increased.
3. After the hot rolling of the slabs and accelerated cooling of the plates, the microstructure consisted of ferrite plus bainite grains with a grain size refinement of $4 \mu\text{m}$ allowing better target properties.

Acknowledgments

The authors acknowledge grant PAPIIT-IN103309 from DGAPA-UNAM. We also thank for the mechanical tests to E. Sanchez.

1. B. De Meester, The weldability of modern structural TMCP steels, *ISIJ International* **37** (1997) 537-551.
2. S. Lee., D. Kwon, Y. K. Lee and O. Kwon, Transformation strengthening by thermomechanical treatments in C-Mn-Ni-Nb steels, *Metall. Mater. Trans.* **36A** (1995) 1093-1100.
3. Y. Shunfa, C. Gouping and C. Meifang, Int. Conf. on "HSLA Steel Metallurgy and Applications" (ASM, Metals Park, OH, 1986) 213-218.
4. K. Hulka, F. Heisterkamp, I. I. Frantov: Int. Conf. on: "An Economic Approach to Pipe Steels with High Toughness and Good

- Weldability, Pipeline Technology*", R. Denys (Ed.), (Antwerpen, Belgium, 1990). pp. 45-65.
5. S. Nemat-Nasser, W. Guo Guo, *Mech. Mater.* **37** (2005) 379-405.
 6. K. Muzka, P. D. Hodgson, and J. Majta, *Mat. Sci. Eng.* **A500** (2009) 25-33.
 7. A. J. DeArdo, *Materials Reviews*, **48** (2003) 371-402.
 8. C. I. Garcia, A. J. DeArdo, E. Raykin, and J. D. S. Defilippi *Steels for Structural Applications*, (Cleveland, OH, USA, 1995). pp. 155-166.
 9. S. Akhlaghi, D. G. Ivey, **41** (2002) 111-119.
 10. A. Ghosha, B. Mishra, S. Dasc, and S. Chatterjee, *Mater. Sci. Eng. A* **396** (2005) 320-332.
 11. M. Charleux, W. J. Poole, M. Militzer and A. Deschamps, *Metall. Mater. Trans.* **36A** (2001) 1635-1647.
 12. S. C. Wang, *J. of Mater. Sci.* **24** (1989) 105-109.
 13. S. S. Hansen, J. B. Vander Sande and M. Cohen, *Metall. Mater. Trans.* **11A** (1980) 387-402.
 14. L. J. Cuddy, *Metall. Mater. Trans.* **12A** (1981) 1313-1320.
 15. P. Choquet, P. Fabregue, J. Giusti, B. Chamont, J. N. Pezant and F. Blanchet: Int. Conf. on "Mathematical Modeling of Hot Rolling of Steel", S. Yue (Ed.), (The Metallurgical Society of CIM, Montreal, Canada, 1990). pp. 34-43.